



ELSEVIER

Available online at www.sciencedirect.com

SCIENCE @ DIRECT®

Journal of Membrane Science xxx (2003) xxx–xxx

**Journal of
MEMBRANE
SCIENCE**

www.elsevier.com/locate/memsci

Evaluation of tantalum-based materials for hydrogen separation at elevated temperatures and pressures[☆]

Kurt S. Rothenberger^{a,*}, Bret H. Howard^a, Richard P. Killmeyer^a,
Anthony V. Cugini^a, Robert M. Enick^b, Felipe Bustamante^b,
Michael V. Ciocco^c, Bryan D. Morreale^{b,c}, Robert E. Buxbaum^d

^a National Energy Technology Laboratory (NETL), US Department of Energy, P.O. Box 10940, Pittsburgh, PA 15236, USA

^b Chemical and Petroleum Engineering Department, University of Pittsburgh, Pittsburgh, PA 15261, USA

^c Parsons Project Services Inc., P.O. Box 618, South Park, PA 15129, USA

^d REB Research and Consulting, Oak Park, MI 48237, USA

Received 20 June 2002; received in revised form 7 January 2003; accepted 28 February 2003

Abstract

The hydrogen permeability of bulk tantalum and tantalum coated with thin films of palladium was measured at temperatures from 623 to 1173 K and hydrogen partial pressures from 0.1 to 2.6 MPa in a flowing gas system. Palladium coatings were deposited by both electroless plating (1–2 μm thick Pd layer) and cold plasma-discharge sputtering with two different thicknesses, 0.04 or 1.2 μm. All samples studied showed declining permeability values with surface fouling over time. The highest absolute values of permeability were observed at the lowest temperatures of study (623–773 K). However, permeability data taken at 1173 K tended to be more consistent with less scatter. The overall trend exhibited declining permeability values as a function of temperature. As confirmed by surface analysis, the palladium coating was lost from the coated tantalum samples. In one test, a 1.2 μm sputter-coated palladium film was observed peeling off the tantalum surface after 49 h at 773 K. The tantalum surface of all tested samples exhibited oxidation, distortion and cracking. Tantalum hydride formation was observed at 623 K, on a palladium sputter-coated sample. Surface fouling limited the hydrogen permeability of all samples studied.

© 2003 Published by Elsevier Science B.V.

Keywords: Tantalum; Hydrogen permeability; Palladium-coated tantalum; High-temperature

1. Introduction

Improved methods for the separation of hydrogen from other gases are a key component of the US De-

partment of Energy's "Vision 21" program. This program is charged with developing the next generation of energy plants with the goal of effectively eliminating, at competitive costs, environmental concerns associated with the use of fossil fuels for producing electricity and transportation fuels. Vision 21 does not describe a specific plant configuration, but rather it outlines a series of technology modules, or options, that would allow a plant to configure to the energy needs and available resources in a given area. However, most Vision 21 configurations incorporate a gasifier, followed at some point by the water-gas-shift re-

[☆] Reference in this paper to any specific commercial product, process, or service is to facilitate understanding and does not necessarily imply its endorsement or favoring by the US Department of Energy.

* Corresponding author. Tel.: +1-412-386-6082;

fax: +1-412-386-4806.

E-mail address: kurt.rothenberger@netl.doe.gov (K.S. Rothenberger).

43 action, resulting in a stream consisting of predomi- 88
 44 nantly hydrogen and carbon dioxide that would require 89
 45 separation. A membrane reactor capable of handling 90
 46 a high-temperature, high-pressure gas stream would 91
 47 greatly benefit Vision 21 in that it would serve the dual 92
 48 purpose of enhancing conversion of carbon monox-
 49 ide by selective removal of hydrogen, and separating
 50 the hydrogen and carbon dioxide products. The ideal
 51 membrane reactor would be capable of functioning in
 52 a high-temperature, high-pressure flowing gas envi-
 53 ronment so as to maximize the efficiencies of the hot,
 54 high-pressure gasifier stream and take advantage of the
 55 more rapid chemical kinetics at high-temperature [1].

56 Tantalum presents an intriguing possibility as a
 57 component in a hydrogen separation membrane. Its
 58 permeability to hydrogen is among the highest of any
 59 pure materials [2]. It is a mechanically tough and
 60 durable material that can easily be incorporated into
 61 a metal infrastructure over a wide temperature range.
 62 It is relatively inexpensive for a specialty metal.
 63 Compared to palladium, it is approximately an order
 64 of magnitude cheaper, and is expected to possess
 65 hydrogen permeabilities approximately an order of
 66 magnitude larger.

67 However, tantalum also has significant shortcom-
 68 ings. One major difficulty is the tendency of tantalum
 69 to form resistant surface oxide layers [3]. This has,
 70 in turn, resulted in a paucity of experimental data on
 71 tantalum-based systems.

72 1.1. Permeability of hydrogen in tantalum

73 The most commonly cited reference for the per-
 74 meability of hydrogen in various materials is a com-
 75 prehensive report by Steward [2]. However, it is in-
 76 structive to note that Steward contains no citation of
 77 experimentally measured hydrogen permeability data
 78 for tantalum. Rather, a correlation is developed, based
 79 on the product of experimentally measured hydrogen
 80 solubility and hydrogen diffusivity data for tantalum.
 81 Specifically, for purposes of the Steward correlation,
 82 the solubility of hydrogen in tantalum was based on
 83 literature data taken from 625 to 944 K, and 0.133 to
 84 106.7 kPa [4], expressed in the form of Eq. (1):

$$86 \quad S(\text{H}_2/\text{Ta}) \text{ (mol/(m}^3 \text{ Pa}^{0.5})) = 0.132 \exp\left(\frac{4050}{T}\right) \quad (1)$$

The diffusivity expression used in the permeability
 correlation was based on a study conducted over a
 lower temperature range of 253–573 K [5]. This ex-
 pression was cited in a critical review [6], and is shown
 in Eq. (2):

$$89 \quad D(\text{H}_2/\text{Ta}) \text{ (m}^2/\text{s}) = (4.4 \times 10^{-8}) \exp\left(\frac{-1620}{T}\right) \quad (2) \quad 92$$

93 The data from this diffusivity study [6] was also in
 94 agreement with the results of a number of other studies
 95 [7–9], none of which went above 573 K. It is interest-
 96 ing to note that the review [6] excluded several sets of
 97 diffusion coefficient data [10–12], that were approxi-
 98 mately 50% lower than the values provided by Eq. (2),
 99 even though these studies covered a wider temperature
 100 range. 101

102 In spite of the lack of overlap in the temperature
 103 ranges, the product of Eqs. (1) and (2) were used to
 104 estimate the hydrogen permeability of tantalum [2], as
 105 expressed in Eq. (3): 106

$$107 \quad k(\text{H}_2/\text{Ta}) \text{ (mol/(m s Pa}^{0.5})) = (5.8 \times 10^{-9}) \exp\left(\frac{2430}{T}\right) \quad (3) \quad 108$$

109 It is further interesting to note that graphical represen-
 110 tations of the correlation in Eq. (3) can be found in the
 111 literature extrapolated to 1000 K [13–16], well above
 112 the range of both the solubility and diffusivity studies.

113 Eq. (3) indicates that the permeability of tantalum
 114 decreases with increasing temperature because the
 115 diffusion coefficient increases with temperature more
 116 slowly than the hydrogen solubility decreases.

117 Measurements of the permeability of hydrogen in
 118 tantalum at high temperatures of 948–1073 K were
 119 reported by Makrides et al. [17] and expressed in the
 120 form of a diffusion constant correlation [6]. This result,
 121 Eq. (4), may be more appropriate for developing a
 122 correlation of high-temperature permeability than the
 123 low temperature correlation, Eq. (2).

$$124 \quad D(\text{H}_2/\text{Ta}) \text{ (m}^2/\text{s}) = (7.5 \times 10^{-6}) \exp\left(\frac{-7290}{T}\right) \quad (4)$$

125 The product of Eqs. (1) and (4) provide an alternate
 expression for the permeability of tantalum in the tem-

126 perature range of 948–1073 K.

$$128 \quad k(\text{H}_2/\text{Ta}) \text{ (mol/(m s Pa}^{0.5}\text{))}$$
$$129 \quad = (1.0 \times 10^{-6}) \exp\left(\frac{-3240}{T}\right) \quad (5)$$

130 Unlike Eq. (3), Eq. (5) indicates that the permeability
131 of tantalum can be expected to increase with increasing
132 temperature because the diffusion coefficient increases
133 with temperature more rapidly than the hydrogen sol-
134 ubility decreases. Despite this difference in trend, the
135 permeability values obtained using Eqs. (3) and (5)
136 differ by a factor of less than 3 over the 948–1073 K
137 temperature range.

138 1.2. Surface contamination

139 Except for the previously cited work of Makrides
140 et al. [17], direct experimental measurements of the
141 hydrogen permeability in tantalum are rare. It is ex-
142 pected that the calculated permeability would be dif-
143 ficult to attain in a real system due to the dominance
144 of surface effects. Unlike palladium, tantalum lacks
145 significant catalytic activity for dissociation of hydro-
146 gen molecules into atoms, a prerequisite for perme-
147 ation through the material. In addition, tantalum tends
148 to form a tenacious surface oxide layer. One author
149 of a diffusion study went so far as to heat a tantalum
150 sample at 2273 K and 6.666×10^2 Pa (5×10^{-10} Torr)
151 in order to remove the surface contamination and re-
152 move the surface resistance [3].

153 To remedy the problem of unfavorable surface ef-
154 fects on permeation, composite membranes have been
155 developed in which tantalum is coated with a thin
156 layer of palladium. In measurements of hydrogen up-
157 take rates on tantalum, it was observed that the depo-
158 sition of even a few monolayers of palladium could
159 dramatically enhance the kinetics of hydrogen disso-
160 lution [18]. In principle, composite membranes would
161 take advantage of the higher permeability, lower cost,
162 and greater mechanical strength of the tantalum core,
163 and the catalytic activity and protection afforded by
164 the thin, non-oxidizing palladium coating. In addi-
165 tion, the performance of a palladium-coated tanta-
166 lum membrane would be less influenced by defects
167 in the coating than would a permeable coating on
168 a porous substrate, as any defect would simply ren-
169 der a minute area of the membrane ineffective rather

170 than causing a leak. Such structures would seem to be
171 economically viable, catalytically active, and durable
172 candidates as membrane materials for high-severity
173 hydrogen separation and membrane reactor applica-
174 tions.

175 Experimental data on a palladium-coated tantalum
176 membrane was first published in the open literature
177 by Buxbaum [13], who used an electroless plating
178 method to deposit a 1–2 μm thick palladium layer on
179 a tantalum disk. This approach was later expanded to
180 tubular membranes and other substrates [14]. These
181 studies employed temperatures from 600 to 700 K at
182 low-to-moderate pressure (20–373 kPa). The perme-
183 ability of the tantalum membranes under these condi-
184 tions was less than the value obtained from Eq. (3).
185 This diminished permeability was attributed to trans-
186 port resistances in the Pd layer, the Pd–Ta interface and
187 the gas phase–Pd boundary. There was a very slight
188 increase in permeability with increasing temperature,
189 although the investigators did not draw any conclu-
190 sions from this trend.

191 The palladium-coated tantalum approach was fur-
192 ther refined by the group of Dye, who performed an
193 ion-etching procedure on thin (approximately 10 μm)
194 tantalum foils followed immediately by sputter coat-
195 ing of palladium, all while the sample was being main-
196 tained under a vacuum of 10^{-4} Pa (10^{-6} Torr) [15,16].
197 This approach insured a highly clean surface as well
198 as deposition of a palladium layer with particular crys-
199 tallographic orientations. In these examples, the mem-
200 brane was studied at temperatures from 573 to 673 K
201 and pressures of 46 and 80–116 kPa. Permeability re-
202 sults were promising, but could not be compared di-
203 rectly with that expected for bulk tantalum, since the
204 palladium represented a significant fraction of the total
205 membrane thickness. The permeability increased with
206 increasing temperature, which was again attributed to
207 the influence of the palladium coating. Interdiffusion
208 of the palladium and tantalum was reported at temper-
209 atures above 673 K.

210 1.3. Objective

211 In summary, tantalum would appear to be a promis-
212 ing material as a component in hydrogen separation
213 membranes operating under high-temperature and
214 high-pressure conditions. However, a number of ques-
215 tions remain unanswered. Although most papers on

216 the topic reference the correlation of Steward [2],
 217 Eq. (3), it is important to remember that it is not based
 218 on experimental permeability, but on experimentally
 219 measured solubility and diffusion coefficients, each
 220 made over limited and non-overlapping temperature
 221 ranges. Experimental measurements of hydrogen per-
 222 meability studies in bulk tantalum or tantalum-based
 223 composite materials are rare and available only in
 224 limited temperature and pressure ranges. Although the
 225 use of palladium coatings has been shown to be effec-
 226 tive in enhancing the performance of tantalum-based
 227 membranes at moderate conditions, it is not known
 228 to what degree such coatings would retain their ef-
 229 fectiveness at elevated temperature and pressure.
 230 Therefore, the objective of this study was to evaluate
 231 the performance of tantalum and palladium-coated
 232 tantalum over a wide range of temperatures (up
 233 to 1273 K) and hydrogen partial pressures (up to
 234 2.6 MPa) characteristic of equilibrium-limited reac-
 235 tions that are candidates for membrane reactors. The
 236 materials studied included bulk (uncoated) tantalum
 237 as well as palladium-coated tantalum fabricated by
 238 both electroless plating and cold plasma sputtering
 239 methods. Steady-state permeation testing in a flowing
 240 configuration was used in combination with surface
 241 characterization of pre- and post-test membranes in
 242 performing the evaluation.

2. Experimental

243

2.1. Membrane fabrication

244

Bulk tantalum membranes were fabricated by 245
 punching 16 mm diameter disks out of a 1 mm thick, 246
 99.9% pure, tantalum sheet (Alfa Aesar). The tanta- 247
 lum disks were mounted in Inconel 600 alloy holders 248
 by one of the two methods: brazing or welding. The 249
 brazing configuration is illustrated in Fig. 1. After 250
 mounting, the tantalum was etched using an acid mix- 251
 ture of 20 vol.% HNO₃, 20 vol.% HF, and 60 vol.% 252
 H₂SO₄ and rinsed with distilled water in order to re- 253
 move surface oxides and contaminants before testing 254
 and/or coating. 255

Tantalum membranes were coated with a thin palla- 256
 dium layer by either electroless plating or cold plasma 257
 sputter coating. *Electroless plating* was done at REB 258
 Research using a deposition technique developed by 259
 Buxbaum and described in a series of published re- 260
 sults [13,14,19,20]. In this procedure, the surface of 261
 the tantalum was roughened and cleaned of oxides and 262
 oil using abrasives and detergent solutions. The tanta- 263
 lum surface was electrolytically hydrided with the 264
 noble metal serving as the cathode. Electroless plating 265
 was used to apply an approximately 1–2 μm thick pal- 266
 ladium film to the tantalum surface, using hydrazine

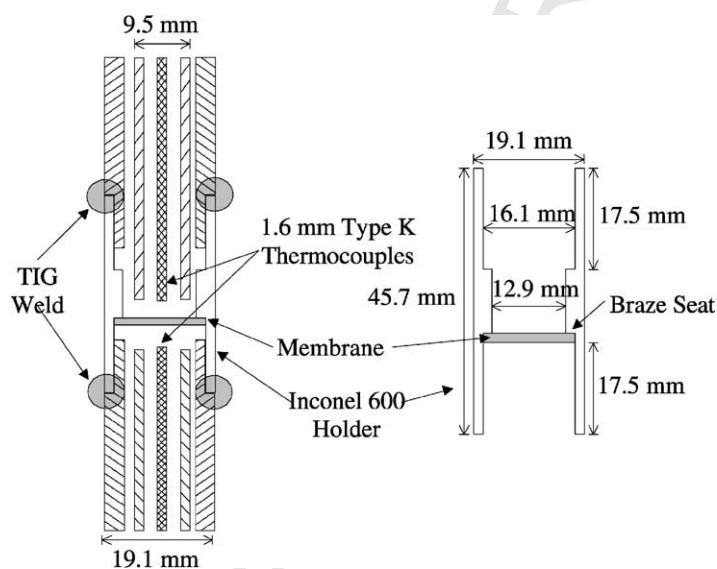


Fig. 1. Schematic of the brazing method used for membrane sealing.

267 as the reducing agent rather than the hypophosphate
268 reported in the literature. The plated metal was heated
269 to enhance the adhesion of the palladium coating.

270 *Cold plasma sputter-coating* was done at the
271 National Energy Technology Laboratory (NETL) using a
272 Denton Vacuum Desk II TSC cold plasma-discharge
273 sputter equipped with a palladium target (Alfa Aesar,
274 99.9% pure). Before sputtering, all surfaces except
275 those to be coated were masked. In a typical coating
276 procedure, the mounted membrane substrate(s)
277 were argon etched for 60 s to remove physisorbed
278 contaminants, and sputtered with palladium in cycles
279 of 999 s until the desired coating thickness, either
280 0.04 or 1.2 μm , was obtained. The process was
281 repeated to coat the second side of the disk. The
282 0.04 μm thickness was verified by performing an
283 X-ray photoelectron spectroscopy (XPS) depth
284 profile. The 1.2 μm coating was verified by
285 calculation based on weight increase and by
286 scanning electron microscopic measurement of
287 the membrane cross-section. For the 0.04 μm
288 coating, XPS indicated that the maximum
palladium thickness was in the center of the
membrane with a decrease

289 in thickness approaching the edge, probably due to a
290 shadowing effect of the holder walls blocking
291 palladium deposition near the edges. This trend is
292 expected to hold for the 1.2 μm coating, but was
not measured.

2.2. Permeability testing

294 The hydrogen membrane testing (HMT) unit was
295 designed and constructed at NETL and has been
296 described previously [1,21]. The apparatus was
297 designed to allow testing of inorganic hydrogen
298 membranes at pressures and temperatures up to
299 3.1 MPa and 1173 K, respectively. A simplified
300 schematic of the HMT unit is illustrated in Fig. 2.
301 The membrane assembly consisted of two 9.5 mm
302 o.d. Inconel 600 tubes, placed concentrically
303 inside the 19.1 mm o.d. Inconel 600 extension
304 tubes, approximately 6 mm from the membrane
305 surface, as shown in Fig. 1. This coaxial tube
306 configuration allowed the feed and sweep gases to
307 enter through the annulus between the 19.1 mm
o.d. and 9.5 mm o.d. tubes, contact the
membrane, and exit through the inside of the
9.5 mm o.d. tube. The mem-

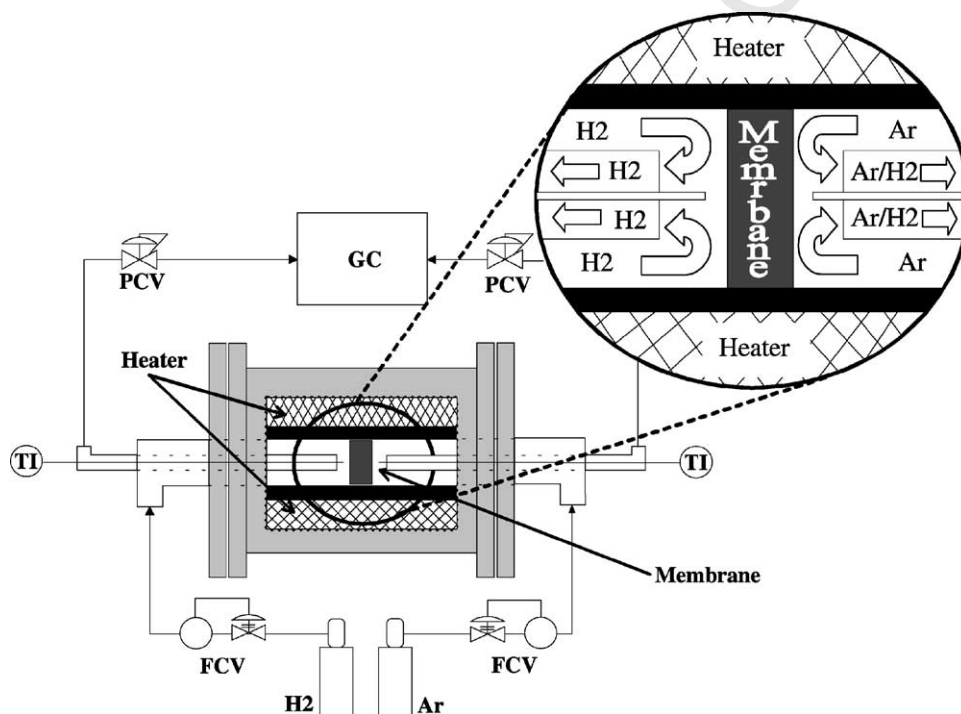


Fig. 2. Schematic of NETL's high-pressure, high-temperature hydrogen membrane testing unit.

brane unit was heated by a Watlow 120 V, 152 mm long concentric resistance heater placed around the membrane assembly. The heater was controlled by an Iconic Genesis process control program, using type-K thermocouples placed approximately 6 mm from both sides of the membrane surface. The membrane unit and resistance heater were insulated with ceramic fiber insulation and housed inside an 8 l stainless steel purge vessel that was continuously flushed with nitrogen. The purge vessel was used to ensure that any fugitive hydrogen evolved from the unit would be diluted, cooled, and vented safely.

The membrane unit feed gas consisted of a mixture of 90% hydrogen and 10% He while ultra-high purity argon was used for the permeate sweep gas. In some cases, the sweep gas was maintained at atmospheric pressure and the total feed pressure equaled the pressure drop. In other cases, the sweep gas was pressurized to minimize the pressure drop across the membranes. Flow rates were controlled by 5850i Series Brooks flow meters, with the feed flow ranging from 190 to 250 sccm and the sweep gas flow controlled so as to maintain the concentration of hydrogen in the permeate at generally less than 4.0 mol%. Water, hydrocarbon and oxygen traps were installed in the reactor gas inlet lines. The feed gas pressure was regulated by a pneumatic, stainless steel, Badger 807 Series Research control-valve. The hydrogen permeating through the membrane was directed to a Hewlett-Packard 5890 Series II gas chromatograph equipped with a 3 m zeolite-packed column and thermal conductivity detector. The detection of helium in the permeate gas was indicative of a membrane leak.

2.3. Permeability calculations

The hydrogen permeation rate through the tantalum membrane was determined as the product of the sweep gas flow rate and the concentration of hydrogen in the sweep gas. The hydrogen flux, N_{H_2} , was obtained by dividing the permeation rate by the surface area of the membrane. Hydrogen permeability was determined by using Eq. (6) to solve for k when the value of the partial pressure exponent, ' n ', was constrained to a value of 0.5.

$$N_{H_2} = \frac{k}{X_M} (P_{H_2,Ret}^n - P_{H_2,Perm}^n) \quad (6)$$

The product of N_{H_2} and membrane thickness, X_M , was divided by $(P_{H_2,Perm}^{0.5} - P_{H_2,Feed}^{0.5})$ yielding hydrogen permeability. When a series of partial pressure data was available, k was determined by plotting N_{H_2} versus $(P_{H_2,Ret}^{0.5} - P_{H_2,Perm}^{0.5})$ and fitting with a line forced through the origin. When more than two points were available, a R^2 "measure of fit" value was also reported. In these cases, a second analysis, based on Eq. (6), was also done in which ' n ' was allowed to float. In this analysis, n and k was derived from the slope and intercept, respectively, of a plot of $\log(N_{H_2})$ versus $\log(P_{H_2,Ret})$. This approach neglected the value of $P_{H_2,Perm}$.

2.4. Characterization techniques

Selected membranes were subjected to surface characterization either prior to or following flux testing (or both). Following testing, membranes were cut out of the extension tubes using a small, dry abrasive blade, taking care to control contamination. The membrane surface was photographed and examined through a stereomicroscope. Advanced instrumental characterization techniques included XPS, X-ray diffraction (XRD), and scanning electron microscopy (backscattered mode) with energy dispersive spectroscopy (SEM/EDS). In some cases, the membranes were cross-sectioned and again analyzed by SEM/EDS.

3. Results and discussion

Tantalum surfaces are well known to be fouled by oxidation and contamination by other impurities. The acid-etching technique described in Section 2 was intended to ameliorate this, so the permeability tests could at least start with a clean surface. XPS depth profiles, taken before and after cleaning, are shown in Fig. 3. Prior to cleaning, oxygen and carbon contamination levels of 10% can still be observed approximately 500 nm into the tantalum surface. Following cleaning, the XPS data shows essentially pure tantalum a few nanometers into the surface. However, it should be noted that the surface itself is still contaminated. This level of contamination is inevitable considering that the sample must be handled in air between the time it is cleaned and when it mounted in the test unit and put under inert gas.

UNCORR

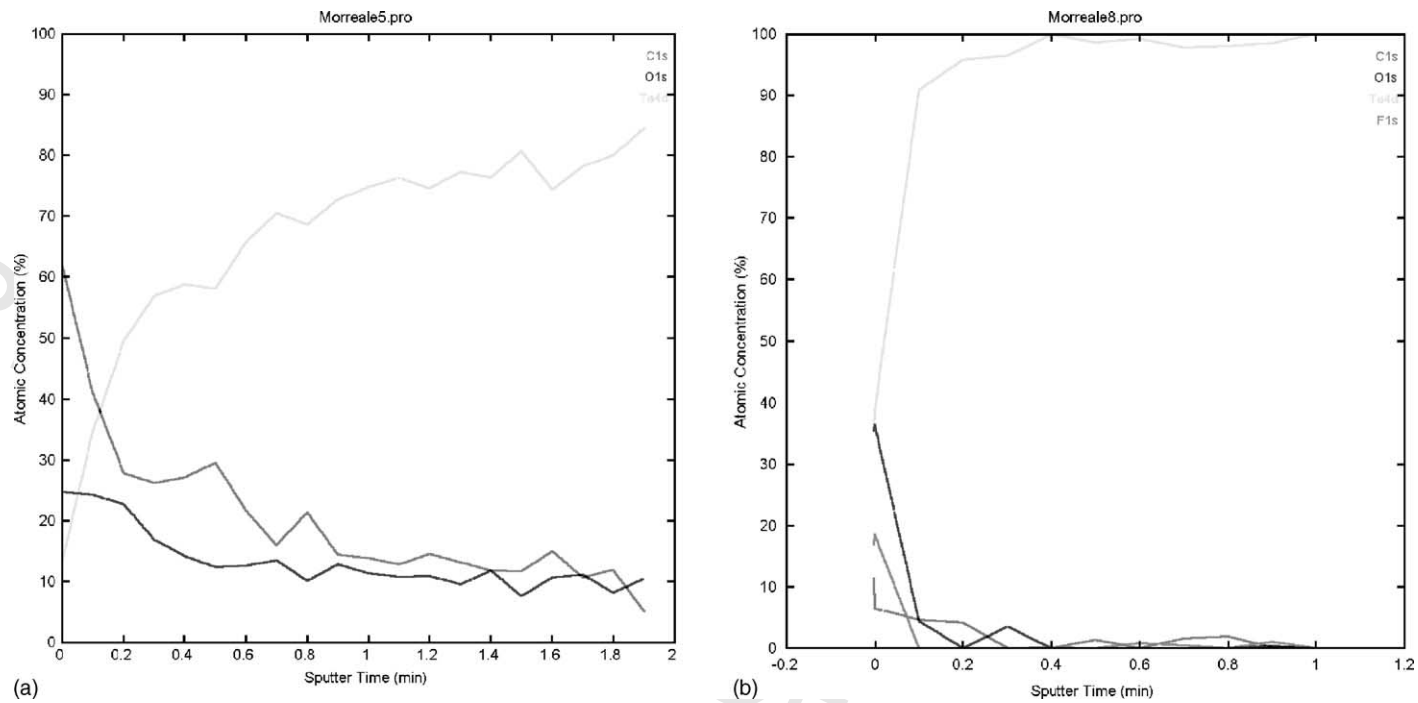


Fig. 3. XPS results on bulk tantalum surface Ta surface (a) before and (b) after “acid-etch” cleaning for 2 min in 20:20:60 nitric:hydrofluoric:sulfuric acid solution (2 min = approx. 0.5 μm in depth).

Table 1
Summary of published literature data for apparent hydrogen permeability ($k \equiv \text{mol/m s Pa}^n$) of tantalum disks

Investigator	X_{Ta} (mm)	X_{Pd} (μm)	T (K)	$P_{\text{Tot,Feed}}$ (kPa)	$P_{\text{H}_2,\text{Feed}}$ (kPa)	$P_{\text{tot,Per}}$ (kPa)	$P_{\text{H}_2,\text{Per}}$ (kPa)	$k \times 10^8$ ($n = 0.5$)	R^2 (of $k \times 10^8$)	$k \times 10^8$ ($n = \rightarrow$)	n	R^2	
1	Ta7 (NETL)	1	0	973	130.6–2910.5	116.0–2585.7	126.4	0.27–3.45	1.73	0.985	0.185	0.65	0.996
2	Ta7 (NETL)	1	0	1073	130.6–2903.6	116.0–2579.5	126	0.25–3.43	1.25–3.71	0.903	0.024	0.77	0.976
3	Ta7 (NETL)	1	0	1173	130.6–2931.5	116.0–2604.4	125.7–126.4	0.54–3.31	1.75	0.976	6.710	0.59	0.966
4	Ta10 (NETL)	1	0	873	106.9–1611.4	94.9–1583.7	125.7–127.1	0.08–1.70	0.94	0.888	0.0054	0.86	0.997
5	Pd/Ta (Buxbaum, 1996)	0.07–0.54	~1	693	101–303	101–303	0–150	0–150	14.50	NA	NA	NA	NA
6	Pd/Ta (Buxbaum, 1996)	NA	~1	682	20–101	20–101	~0	~0	11.00	NA	NA	NA	NA
7	Pd/Ta (Buxbaum, 1996)	NA	~1	697	20–101	20–101	~0	~0	13.00	NA	NA	NA	NA
8	Pd/Ta (Buxbaum, 1993)	2	2	616	373	280	101	5	7.50	NA	NA	NA	NA
9	Pd/Ta (Buxbaum, 1993)	2	2	630	373	280	101	5	7.90	NA	NA	NA	NA
10	Pd/Ta (Buxbaum, 1993)	2	2	644	373	280	101	5	8.80	NA	NA	NA	NA
11	Pd/Ta (Buxbaum, 1993)	2	2	658	373	280	101	5	9.80	NA	NA	NA	NA
12	Pd/Ta (Buxbaum, 1993)	2	2	671	373	280	101	5	10.70	NA	NA	NA	NA
13	Pd/Ta (Buxbaum, 1993)	2	2	686	373	280	101	5	11.60	NA	NA	NA	NA
14	Pd/Ta-electroless (NETL)	1	~1	623	106.2–106.9	94.3–94.9	127.1	0.66–0.71	1.92	NA	NA	NA	NA
15	Pd/Ta-electroless (NETL)	1	~1	923	106.2–2910.5	94.3–2585.7	125.0–127.1	0.04–0.77	0.12–0.58	0.793	0.0044	1.01	0.996
16	Pd/Ta-electroless (NETL)	1	~1	1173	106.2–1248.2	94.3–1108.9	125.7–127.1	0.14–0.18	0.38–0.39	0.911	5.95	0.46	0.896
17	Pd/Ta1-sputter (NETL)	1	~0.04	623	106.2	94.3	127.1	1.81	4.65	NA	NA	NA	NA
18	Pd/Ta2-sputter (NETL)	1	~0.04	623	104.8	93.1	127.1	3.42	12.6	NA	NA	NA	NA
19	Pd/Ta3-sputter (NETL)	1	~0.04	1173	117.0–123.0	104.9–111.1	140.0–141.0	0.69–0.74	1.83–2.28	NA	NA	NA	NA
20	Pd/Ta4-sputter (NETL)	1	~0.04	923	122.3–2845	110.0–2560	143.8–2886	0–1.63	0.04–3.88	NA	NA	NA	NA
21	Pd/Ta4-sputter (NETL)	1	~0.04	1173	120.7–2859	108.6–2573	142.7–2887	0.58–13.2	0.22–2.76	NA	NA	NA	NA
22	Pd/Ta10-sputter (NETL)	1	~0.04	623	200.6	180.5	161.3	3.44	6.38	NA	NA	NA	NA
23	Pd/Ta6-sputter (NETL)	1	~1.2	923	136.9–2896.6	123.2–2606.9	138.9–2896.6	0.22–121.22	1.16	0.954	0.108	0.65	0.997
24	Pd/Ta7-sputter (NETL)	1	~1.2	1173	139.7–140.4	125.7–126.4	138.3–139.7	2.00–2.73	1.43–2.40	NA	NA	NA	NA
25	Pd/Ta8-sputter (NETL)	1	~1.2	773	158.6–940.9	142.7–846.8	151.6–865.4	3.11–36.24	6.33–8.55	0.995	649.0	0.44	0.995

395 3.1. Bulk tantalum

396 The first bulk, uncoated tantalum membrane, des-
397 ignated as Ta7 in summary Table 1, was tested for
398 hydrogen permeability for 10 days at temperatures
399 from 873 to 1173 K and pressure drops from atmo-
400 spheric to 2.8 MPa. Equilibration times were slow,
401 particularly at the beginning of the test. On day 3
402 of testing, two points, at pressures of approximately
403 0.1 and 0.6 MPa, were recorded at a temperature of
404 1073 K. These points yielded a permeability of $3.7 \times$
405 10^{-8} mol/(m s Pa^{0.5}), or 66% of the value predicted
406 from the Steward correlation.

407 During the 6th and 7th days of testing, a series
408 of four partial pressure conditions ranging from
409 0.1 to 2.6 MPa were measured at 973 K. These
410 values yielded consistent permeability values of
411 1.7×10^{-8} mol/(m s Pa^{0.5}) ($R^2 = 0.985$) or only
412 25% of that predicted from the Steward correlation.
413 Whether this decline in permeability was due to the
414 decline in temperature or to fouling of the membrane
415 with time could not be determined. However, it was
416 noted that the data at this temperature could be better
417 fit ($R^2 = 0.996$) using an exponent of $n = 0.65$, indicat-
418 ing that surface effects may have influenced the
419 permeability behavior.

420 During day 8 and again on day 10, data taken at
421 1173 K at pressures from 0.1 to 2.6 MPa partial pres-
422 sure hydrogen were less consistent, although the dif-
423 ferences in data taken on the different days was fairly
424 minor. Overall, permeability corresponded to a value
425 of 1.7×10^{-8} mol/(m s Pa^{0.5}) ($R^2 = 0.976$), essentially
426 the same as that measured at 973 K. However, due to
427 the decreasing nature of the Steward correlation with
428 temperature, this value was 38% of that predicted from
429 the Steward correlation. A better fit of the data could
430 not be obtained by allowing the exponent, n , to float,
431 making it difficult to determine whether the 1173 K
432 permeability was influenced by surface effects.

433 During days 8 and 9, the 1073 K temperature con-
434 dition was repeated, only with a wider range of partial
435 pressures, from 0.1 to 2.6 MPa. The decline in mem-
436 brane performance over time was dramatically evi-
437 denced by this result. Although the data contained sig-
438 nificant scatter, the best fit permeability corresponded
439 to a value of 1.3×10^{-8} mol/(m s Pa^{0.5}) ($R^2 = 0.903$),
440 only 34% of the value measured during the first 3 days
441 of testing and 22% of that predicted from the Steward

442 correlation. The fit could be improved ($R^2 = 0.976$)
443 using an exponent of $n = 0.77$, indicating that surface
444 effects likely influenced the measured permeability.

445 A second bulk tantalum sample, designated Ta10
446 in Table 1, was tested for a 4-day period, at 873 K
447 and hydrogen partial pressures from 0.1 to 1.6 MPa
448 before a failure occurred. Measured permeability cor-
449 responded to a value of 0.94×10^{-8} mol/(m s Pa^{0.5})
450 ($R^2 = 0.888$) or only a 10th that predicted from the
451 Steward correlation. The poor fit most likely was a re-
452 sult of artificially forcing the data to an exponent of
453 $n = 0.5$. When allowed to float, a value of $n = 0.86$
454 improved the fit significantly ($R^2 = 0.997$), indicat-
455 ing that this sample was dominated by surface effects,
456 and that the k for $n = 0.5$ is probably not valid.

457 Surface analysis of the tantalum after testing clearly
458 demonstrated that both membranes became contam-
459 inated over the course of the tests. XPS analysis of
460 post-test tantalum (Fig. 4) showed carbon and oxygen
461 levels of up to 20% at least 150 nm into the surface.
462 This level of contamination was at least as severe as
463 had existed in the sample before acid etching. It is pos-
464 sible that the high temperatures of testing caused some
465 of the surface contaminants to diffuse further into the
466 bulk material, resulting in a temporarily cleaner sur-
467 face, but deeper bulk contamination.

468 SEM was also used to probe changes in surface
469 features that occurred upon exposure to the high tem-
470 peratures, pressures, and gas flows during the testing
471 process. Following the acid etching process, some sur-
472 face contour could be observed as a result of disso-
473 lution of surface Ta oxides and metal, as shown in
474 Fig. 5a. Following testing, the surface showed a vari-
475 ety of changes. Specific changes observed depended
476 on the maximum temperature, exposure duration, pres-
477 sure drop across the membrane, and the side of the
478 membrane (feed versus permeate) under examination.
479 All bulk tantalum membranes analyzed after testing
480 showed some degree of surface oxidation ranging from
481 minor to extreme. Examples are shown in Fig. 5b–d.

482 The tantalum membrane pictured in Fig. 5b and c
483 showed significant surface oxidation on the feed side
484 and slightly less on the permeate side. Oxidized areas
485 are seen as dark features in these images. A crack
486 associated with the failure is visible in Fig. 5b. On the
487 permeate side, evidence of surface restructuring was
488 observed as a triangular pattern probably caused by
489 tensional stretching of the surface due to distortion of

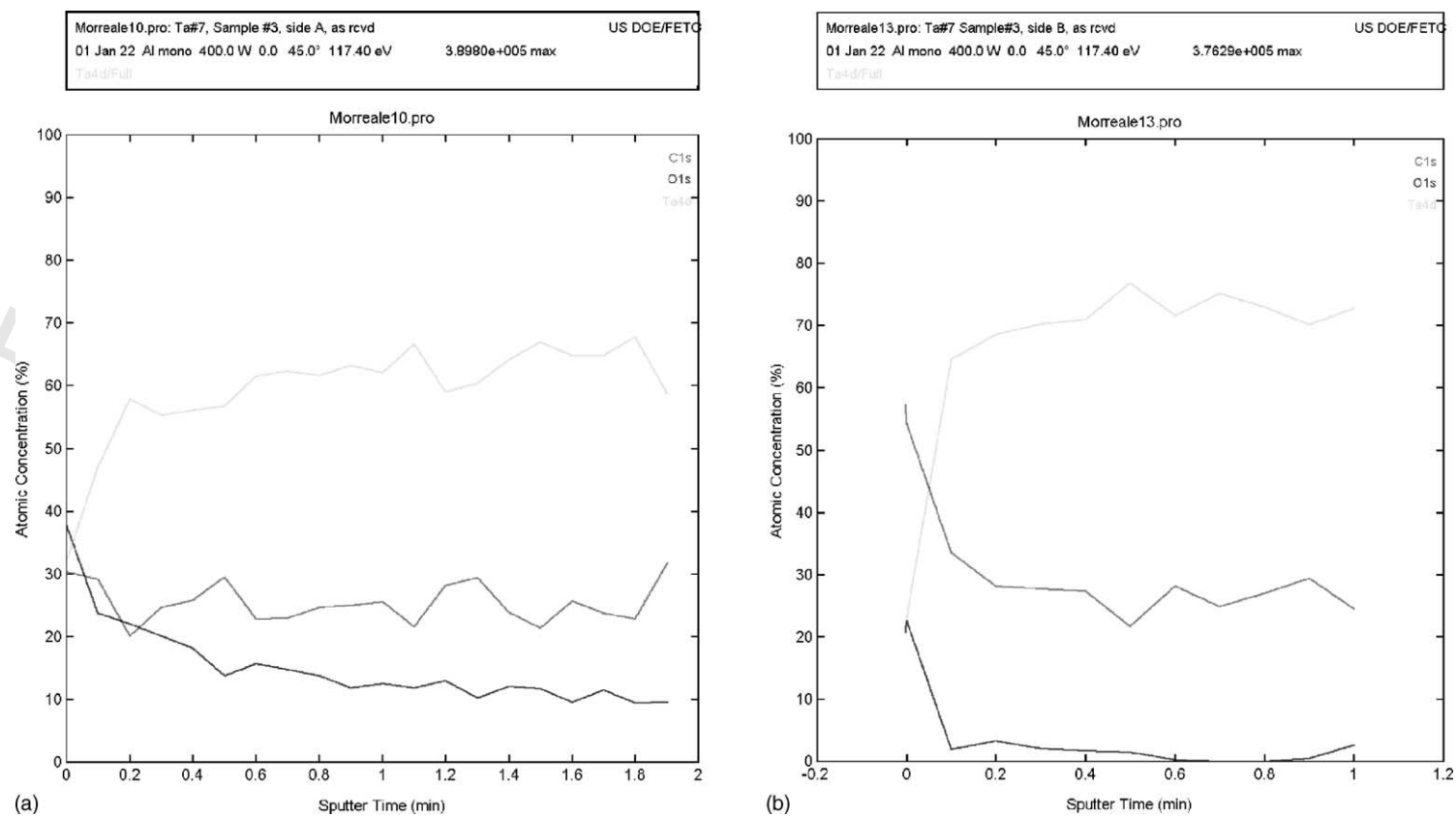


Fig. 4. XPS data on tantalum membrane after testing. Example (a) shows atomic carbon and oxygen concentrations of approximately 20 and 10%, respectively, at least 150 nm into membrane. Example (b) shows carbon atomic concentration of approximately 30% deep into membrane surface.

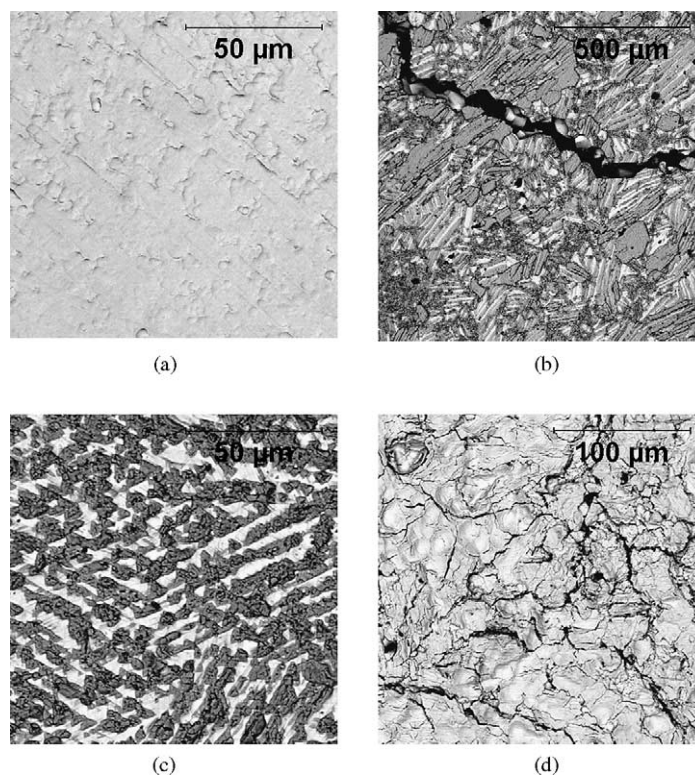


Fig. 5. SEM analysis of pre- and post-tested bulk tantalum membranes. (a) Fresh, chemically etched Ta surface showing pitting due to removal of material from the surface. (b) Feed side of post-test bulk tantalum surface showing oxidized (dark) features and crack associated with membrane failure. (c) Permeate side of post-test bulk tantalum surface showing triangular pattern indicative of tensional stretching. (d) Feed side of post-test bulk tantalum membrane showing cracking in surface.

490 the membrane. Oxide growth occurred preferentially
 491 at these disturbances resulting in regular tantalum oxide
 492 islands.

493 The membrane pictured in Fig. 5d was tested to
 494 2.6 MPa at 1173 K. Unlike the membrane in Fig. 5b
 495 and c, this membrane exhibited no oxide phase separation.
 496 XPS depth profiling (Fig. 4) suggested the presence of
 497 carbide formation on the surface in addition to oxide.
 498 For this membrane the C and O was probably dissolved
 499 into the Ta metal. Cracking of the membrane was again
 500 seen, even though no failure occurred with this sample.
 501 The surface contamination seen in these figures most
 502 likely accounted for the drop in permeability observed
 503 after the initial 1073 K readings.
 504

505 The bulk tantalum permeability results are summarized
 506 in Table 1 and Fig. 6. Table 1 also provides information
 507 on the membrane dimensions and the con-

ditions associated with tantalum permeability values
 508 both for the NETL results and from published literature
 509 data. Fig. 6 illustrates tantalum permeability as a
 510 function of inverse temperature. Overall permeability
 511 results for bulk tantalum overlapped those published
 512 by Makrides et al., which had been measured over a
 513 similar but narrower temperature range. The temperature
 514 dependence of the NETL data was scattered, but
 515 showed a slight trend to higher permeability at
 516 increased temperature, in agreement with that recorded
 517 by Makrides and opposite that predicted by Steward.
 518 Surface resistances plainly developed over time due
 519 to oxidation or contamination of the tantalum surfaces
 520 in the high-pressure, continuous-flow permeation unit.
 521 However, it also appears that surface contamination
 522 may have had a greater impact at lower temperature,
 523 thus providing some bias toward higher permeability
 524 values with increasing temperature.
 525

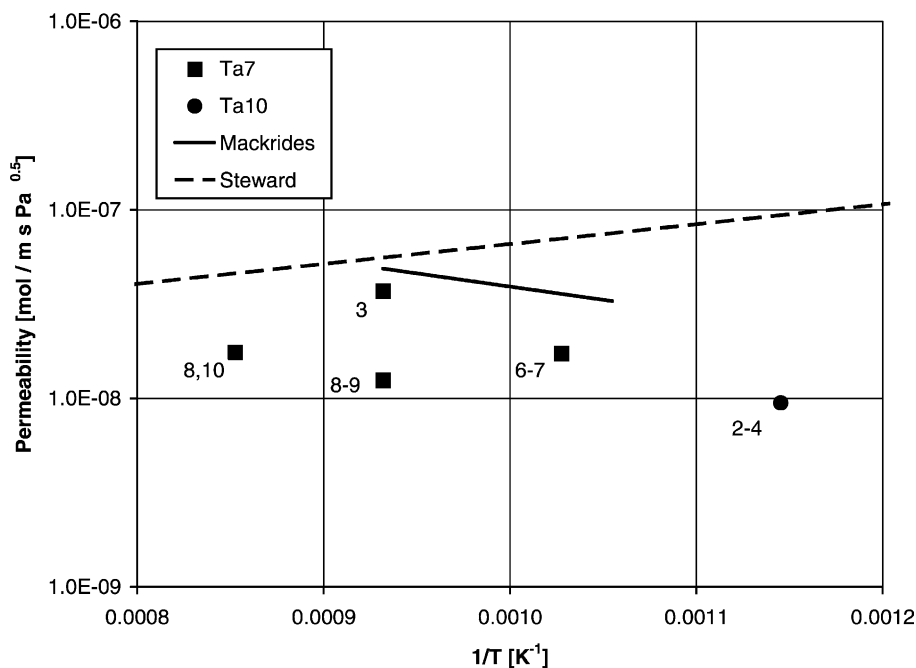


Fig. 6. Hydrogen permeability results in bulk tantalum samples. Numbers in the legend correspond to membrane designations in the text and Table 1. Numbers near the data represent the number of days into test that the data point was acquired.

526 3.2. Electroless-plated palladium-coated 527 tantalum

528 Two electroless-plated palladium-coated tantalum
529 membranes were prepared. One was saved for char-
530 acterization, while the other was tested for 28 days,
531 the longest single test of any tantalum-based mem-
532 brane. During this time, it was subjected to temper-
533 atures of 623, 923, and 1173 K, and pressure drops
534 up to 2.8 MPa. Equilibration times were extremely
535 slow during the initial portion of the test. The first
536 17 days of testing were required to obtain just three
537 conditions, atmospheric pressure at each of the three
538 temperatures, with each condition requiring several
539 days to reach steady-state operation. The initial con-
540 dition, at 623 K, exhibited a slow increase in flux to
541 an asymptotic value corresponding to a permeability
542 of 1.9×10^{-8} mol/(m s Pa^{0.5}) on days 6–8. Each of the
543 changes to higher temperature was met by an initial
544 outgassing of hydrogen followed by an equally slow
545 decrease in flux, again to an asymptotic value, with
546 permeabilities of 0.58×10^{-8} mol/(m s Pa^{0.5}) at 923 K
547 on day 9, and 0.38×10^{-8} mol/(m s Pa^{0.5}) at 1173 K

548 on days 15–17. Each of these values is about 10% of
549 that predicted by the Steward correlation. However,
550 the slope of the line formed from these three initial
551 points is nearly parallel to that of Steward.

552 Following exposure to 1173 K, equilibration times
553 became considerably quicker, similar to that observed
554 with the bulk tantalum samples, but measured perme-
555 abilities dropped. A return to the temperature of 923 K
556 during days 19–20 of the test resulted in a permeabil-
557 ity of 0.12×10^{-8} mol/(m s Pa^{0.5}), only 20% of its day
558 9 value and less than 2% of that predicted by Steward.
559 The temperature was then raised again to 1173 K and,
560 during days 21–26, limited pressure data was recorded
561 from 0.1 to 1.1 MPa. Permeability values, which
562 should have remained constant during this pressure
563 sequence (assuming that the choice of $n = 0.5$ was a
564 valid exponent), actually declined a total of 30% (from
565 0.46×10^{-8} to 0.33×10^{-8} mol/(m s Pa^{0.5})) through-
566 out this test sequence, indicating that the membrane
567 was degrading over time. Overall, the “best fit” per-
568 meability for $n = 0.5$ was 0.40×10^{-8} mol/(m s Pa^{0.5})
569 ($R^2 = 0.911$). The fit could not be improved by a
570 different choice of the exponent, n .

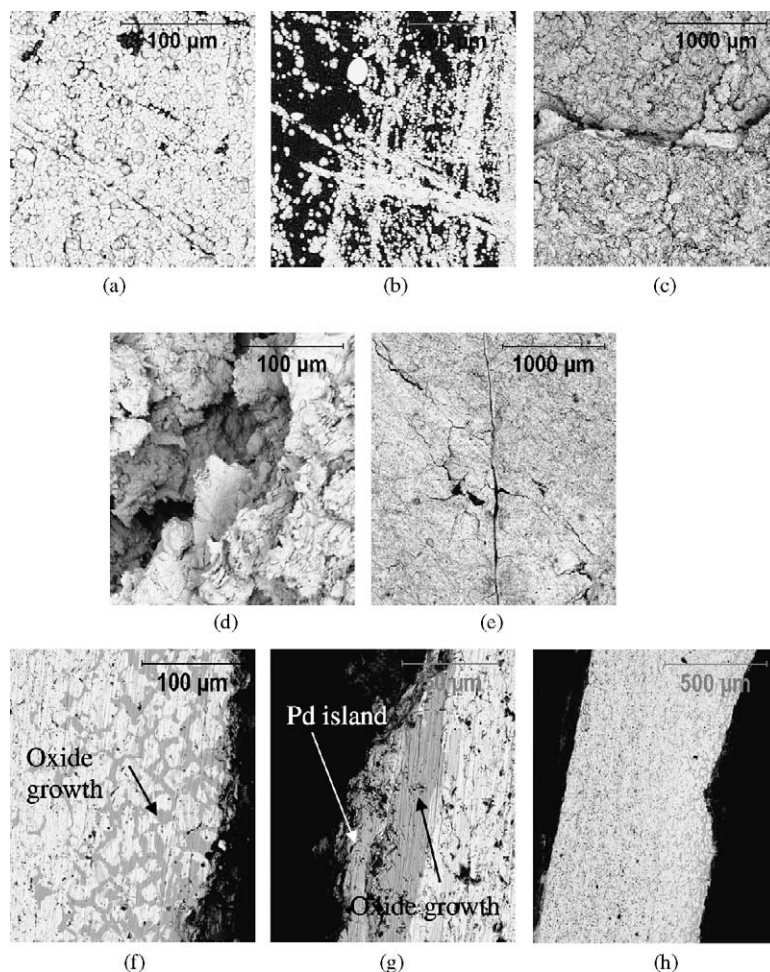


Fig. 7. SEM analysis of tantalum sample coated with 1–2 μm palladium via electroless plating. (a) Area of high Ta coverage on as-received membrane. (b) Area of low Ta coverage on as-received membrane. (c) Retentate side of membrane after testing showing surface damage. (d) Detail of the retentate side of the membrane after test. (e) Permeate side of the membrane after test showing surface damage and cracking. (f) Cross-sectional view of oxide growth into the retentate side of the membrane after test. (g) Cross-sectional view of residual palladium island and oxide growth on the permeate side of the membrane after test. (h) Cross-section of the membrane showing material loss from retentate side after test.

571 During days 27–28, a pressure study from 0.1 to
 572 2.6 MPa was made at 923 K. Unlike the 1173 data,
 573 permeability values increased, rather than declined,
 574 over this pressure range. When forced to $n = 0.5$, the
 575 best fit permeability was $0.36 \times 10^{-8} \text{ mol}/(\text{m s Pa}^{0.5})$
 576 ($R^2 = 0.793$). A much better fit could be obtained
 577 with $n = 1.0$ ($R^2 = 0.996$), indicating that the mem-
 578 brane permeability was completely governed by sur-
 579 face effects at this point in the test.

Two electroless palladium-plated membranes were 580
 characterized—one in a freshly prepared state and the 581
 other following nearly a month of testing. The freshly 582
 prepared membrane, Fig. 7a and b, was fabricated by 583
 the same method as the membrane tested but was not 584
 mounted in a holder. This membrane had an estimated 585
 80% palladium coverage on one side and significantly 586
 less on the other. The Pd had a globular appearance 587
 possibly due to growth from individual surface nu- 588

589 cleation sites. Individual globular regions were about
590 10 μm in diameter. There also appeared to be some
591 linear associations of the Pd spheres which may have
592 been due to growth nucleation aligned with surface
593 scratches.

594 Microscopic examination of the electroless-plated
595 membrane that was removed from the reactor after
596 nearly a month of testing indicated that both the feed
597 and sweep sides had been highly altered during mem-
598 brane testing. Both sides were dark colored and rough
599 with visible surface cracking. There was no visible
600 evidence of palladium.

601 SEM/EDS results, Fig. 7c–e, suggested that the tan-
602 talum surface was oxidized and that material loss was
603 due to spalling of this oxide layer. The surface spalling
604 would also have removed the palladium coating. A
605 small amount of residual palladium was found on the
606 permeate side of the membrane although this palla-
607 dium appeared very porous and poorly bound to the
608 surface. The extreme duration of this test run as com-
609 pared to others in this study accounts for the signifi-
610 cant oxidation effects observed.

611 The used electroless-plated membrane was also
612 cross-sectioned and analyzed by SEM/EDS. Exami-
613 nation of the feed side indicated that a tantalum oxide
614 phase had formed in the membrane's surface, ap-
615 parently forming along grain boundaries. This oxide
616 formation extended up to 200 μm into the surface,
617 Fig. 7f.

618 The permeate side did not show this extreme ox-
619 ide formation extending into the membrane surface.
620 Also, there were some areas that showed residual
621 Pd coating. One of these areas is shown in Fig. 7g.
622 Examination of this Pd coated area indicated that
623 the coating consisted of a somewhat porous $\approx 10 \mu\text{m}$
624 Pd layer containing some Ta and C over a simi-
625 lar thickness oxygen-enriched Ta layer over bulk
626 Ta.

627 Also apparent from the cross-section, Fig. 7h, was
628 that the membrane lost a large amount of material from
629 the surface, primarily on the feed side, resulting in a
630 reduction in thickness by about 25%. As stated ear-
631 lier, this material loss was probably caused by spalling
632 resulting from surface oxidation. The surface spalling
633 would account for the loss of the palladium coating.
634 The duration of this test run as compared to others in
635 this study accounts for the extreme oxidation effects
636 observed in this membrane.

637 The evolution of permeability values for the
638 electroless-plated palladium-coated tantalum mem-
639 brane are shown in Table 1 and graphically in Fig. 8.
640 These results were approximately an order of mag-
641 nitude below both the Steward correlation and the
642 data of Buxbaum and Marker [13] and Buxbaum and
643 Kinney [14], although the temperature dependence of
644 the permeability was fairly close to that predicted by
645 Steward [2]. This latter fact may simply have been a
646 result of membrane degradation over time. Due to the
647 difficulties involved in preparing a sample at one site,
648 coating it at another, and sending it back for mount-
649 ing and testing, it is likely that the electroless-plated
650 membrane was contaminated before the permeability
651 test even started. The characterization data, together
652 with permeability behavior, likely represents a con-
653 secutive series of stages involving loss of the palla-
654 dium coat, fouling of the tantalum surface, spalling
655 of the oxide layer, followed by additional fouling and
656 loss of material.

657 3.3. Sputter-coated tantalum

658 As a result of difficulties encountered with the han-
659 dling of the electroless-plated palladium over tanta-
660 lum, it was thought that better quality control could be
661 gained from a coating procedure done at one location.
662 Using the sputter coating method, the bulk tantalum
663 metal was acid etched, placed in a vacuum chamber
664 and ion-etched, then sputtered with palladium without
665 removal from the chamber or exposure to air, very simi-
666 lar to that described in references [15,16]. Represent-
667 ative tantalum membranes sputter-coated with palla-
668 dium were characterized before testing. For both pal-
669 ladium thicknesses, 0.04 and 1.2 μm , the surface mor-
670 phology was not altered from that of the etched tan-
671 talum substrate. All coatings characterized appeared
672 highly uniform.

673 A series of five test runs (PdTa1, 2, 3, 4, and 10
674 in Table 1) were made using the bulk tantalum disk
675 sputter-coated on each side with a "thin" (average
676 thickness = 0.04 μm) palladium film. In these tests,
677 the sweep pressure was increased to minimize the pres-
678 sure drop across the membrane. In this configuration,
679 the partial pressure gradient is dependent on main-
680 taining an adequate sweep flow to keep the concen-
681 tration of hydrogen in the sweep gas low. PdTa1, 2,
682 and 10 were tested at 623 K and atmospheric pressure.

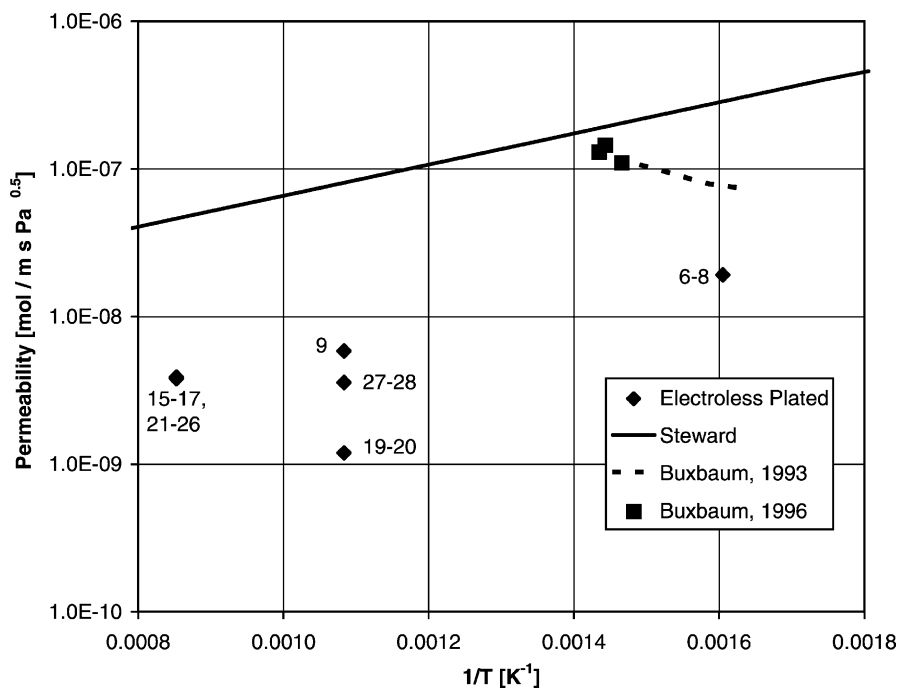


Fig. 8. Evolution of the hydrogen permeability of electroless-plated palladium-coated tantalum sample. Numbers in the legend correspond to membrane designations in the text and Table 1. Numbers near the data represent the number of days into test that the data point was acquired.

683 These runs yielded permeability values of 4.6×10^{-8} ,
 684 13×10^{-8} , and 6.4×10^{-8} mol/(m s Pa^{0.5}), respectively.
 685 Neglecting any contributions from the palladium film
 686 coating, these values are 16, 44, and 22% of the value
 687 predicted from the Steward correlation, and also pro-
 688 vide a good indication of the level of variability of
 689 samples prepared using an essentially identical proce-
 690 dure. The value of 13×10^{-8} mol/(m s Pa^{0.5}) was the
 691 highest permeability measured on any tantalum-based
 692 membrane during this series of tests. In each of the
 693 tests, the membranes failed upon attempting to change
 694 temperature or pressure conditions.

695 Of the remaining two samples with the thin
 696 sputter-coated palladium film, PdTa3 was tested at
 697 atmospheric pressure at 1173 K. Over a 48 h period,
 698 this sample showed an initial increase in flux to a
 699 maximum value corresponding to a permeability of
 700 2.3×10^{-8} mol/(m s Pa^{0.5}) (50% of the value pre-
 701 dicted by Steward) followed by a slow decline to
 702 a steady-state value of 1.8×10^{-8} mol/(m s Pa^{0.5})
 703 (40% of the Steward correlation). PdTa4 was cycled

704 from 923 to 1173 K and back to 923 K at pressures
 705 from 0.1 to 2.6 MPa hydrogen over a 10-day pe-
 706 riod. This sample showed continuously degrading
 707 permeability behavior over the course of the test.
 708 Permeability at 923 K declined from an initial value
 709 of 3.9×10^{-8} mol/(m s Pa^{0.5}) (48% of Steward) on
 710 day 1 to 0.04×10^{-8} mol/(m s Pa^{0.5}) (<1% of Stew-
 711 ard) on day 10. Permeability at 1173 K declined from
 712 an initial value of 2.8×10^{-8} mol/(m s Pa^{0.5}) (60%
 713 of Steward) on day 3 to 0.29×10^{-8} mol/(m s Pa^{0.5})
 714 (6% of Steward) on day 9. No pressure dependence
 715 of the permeability could be determined due to the
 716 continuously degrading nature of the results.

717 After testing, no palladium could be detected on the
 718 surfaces of any of the “thin” sputter-coated membranes
 719 by XPS. Some oxidation was evident and carbon de-
 720 position was also observed. In the case of the three
 721 membranes that cracked after exposure to hydrogen at
 722 623 K, hydride formation was suspected. However, it
 723 could not be detected by XRD for samples PdTa1 and
 724 2. It turned out that the tantalum hydride phase was

725 reconverting to tantalum metal upon cool down of the
 726 samples, which is usually done under inert gas follow-
 727 ing a membrane failure. In the PdTa10 test, a hydro-
 728 gen atmosphere was maintained during the cool down
 729 period. Only then was the tantalum hydride phase con-
 730 firmed by XRD.

731 Permeability values and trends are shown in Table 1
 732 and in the plot of Fig. 10. All the points fell below the
 733 line predicted by the Steward correlation, but were
 734 much higher than those that had been obtained with
 735 the NETL electroless-plated sample. Interestingly, the
 736 values were similar to those reported by Buxbaum
 737 and coworkers in their own permeability studies of
 738 electroless-plated palladium-coated tantalum in the
 739 range of 600–700 K [13,14]. Taken together with
 740 the characterization data, the results depict a scen-
 741 ario where the initial permeability was high when
 742 the palladium coating was fresh (and likely intact).
 743 In the samples tested at 623 K, the concentration of
 744 hydrogen in the tantalum was high enough to form
 745 a hydride phase either before, or concomitant with,
 746 the loss of the palladium coating. In the samples
 747 examined from 923 to 1173 K, the permeability was
 748 not high enough to form a hydride. Instead, after the
 749 protective palladium coating was lost, the membrane
 750 fouled, and the permeability declined.

751 Subsequently, a series of three test runs, with sam-
 752 ple designations PdTa6, 7, and 8 in Table 1, were made
 753 using bulk tantalum disks sputter-coated on each side
 754 with a “thick” (average thickness = 1.2 μm) palla-
 755 dium film. The goal of these experiments was to see if
 756 the palladium film thickness improved the durability
 757 of the sample or otherwise influenced the permeation

758 behavior. Each test was limited to a single temperature
 759 to simplify the interpretation of characterization data.
 760 PdTa6 was tested at 923 K over 4 days. The sample
 761 was subjected to a complete pressure sequence from
 762 0.1 to 2.6 MPa without any obvious degradation of
 763 the membrane over time. The permeability equation
 764 was fit to a value of $1.2 \times 10^{-8} \text{ mol}/(\text{m s Pa}^{0.5})$ ($R^2 =$
 765 0.954), 15% of that predicted by Steward. However,
 766 a better fit could be obtained using $n = 0.65$ ($R^2 =$
 767 0.996), indicating that surface resistances may have
 768 been present under these conditions.

769 PdTa7 was tested for 48 h at 1173 K and atmo-
 770 spheric pressure. Measured permeability rose to a
 771 maximum of $2.4 \times 10^{-8} \text{ mol}/(\text{m s Pa}^{0.5})$ (52% of
 772 Steward) in hour 13, then declined to a “steady-state”
 773 value of $1.4 \times 10^{-8} \text{ mol}/(\text{m s Pa}^{0.5})$ (31% of Stew-
 774 ard) by the end of the test. In spite of the thicker,
 775 1.2 μm -coating, the palladium was nearly gone from
 776 both the feed and permeate surfaces of both PdTa6
 777 and 7 after testing at 923 and 1173 K, respectively.
 778 Some minor oxidation and carbon deposition was
 779 noted. The lower degree of oxidation seen for these
 780 membranes versus previous tests was most likely due
 781 to the relatively short run duration. The limited palla-
 782 dium that was observed usually had a highly porous
 783 morphology. One of these residual porous-appearing
 784 palladium islands remaining on the feed side of the
 785 membrane after the 1173 K test is shown in Fig. 9a.

786 The PdTa8 test was designed as a short duration
 787 lower temperature exposure in an attempt to pre-
 788 serve the palladium coating. It took place at 773 K
 789 over 49 h. The sample showed continuous, but slow
 degradation of permeability from initial to final read-

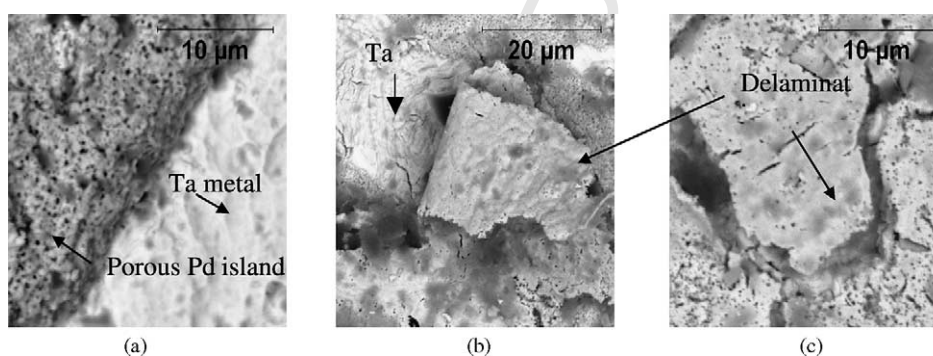


Fig. 9. SEM analysis of post-tested palladium-coated tantalum membrane. (a) Membrane detail showing porous palladium island remaining on tantalum substrate after 1173 K test. (b) and (c) Detail showing cracked and peeling porous palladium layer after 49 h at 773 K.

ings, from 8.6×10^{-8} to 6.5×10^{-8} mol/(m s Pa^{0.5}) in 5–8 h to 6.3×10^{-8} mol/(m s Pa^{0.5}) in 48–49 h (64–48% of Steward), with both values recorded at atmospheric pressure. A limited pressure sequence (from 0.1 to 0.9 MPa) was performed midway through the test. Only data taken during a consecutive 8 h period was included in the pressure sequence so as to minimize the effects of membrane degradation. This data was well fit by a permeability expression of 7.7×10^{-8} mol/(m s Pa^{0.5}) ($R^2 = 0.995$), 63% of Steward, and consistent with the pace of degradation over the course of the test. The fit could not be improved with the choice of a different exponent, n .

Post-test examination via SEM revealed a highly interesting observation. Palladium remained on both surfaces of the 773 K test sample. However, the palladium layer appeared cracked and porous with some areas peeling off exposing tantalum. It appeared that the conditions under which the palladium coating was lost, as well as the mechanism of its failure, had been successfully elucidated. Examples are shown in Fig. 9b and c.

The recorded permeability ranges, again with ‘ n ’ constrained to 0.5, are listed in Table 1 and Fig. 10.

Taken as a group, the permeability values for both the “thin-Pd” and “thick-Pd” sputter-coated membranes fall within a range below that predicted by the Steward correlation, although many samples evidenced initial maximum readings (before degradation set in) that approached the Steward line within a factor of two. Although the highest absolute permeability values were recorded at temperatures of 723 K or less, the smaller variations in the measured permeability tended to occur at higher temperatures. This may also indicate that surface effects are less important at the highest temperatures; perhaps impurities diffuse away from the tantalum surface into the bulk material, providing at least temporary cleaning.

Based on the characterization of the fresh and tested sputter-coated membranes, particularly that for the PdTa8 sample, the palladium losses observed following testing were most likely due to delamination of the palladium layer. Although the loss of the palladium layer at elevated temperatures comes as no surprise, the mechanism was unexpected. In a previous literature reference, interdiffusion, or alloying, was cited as a cause for degradation of a sputter-coated

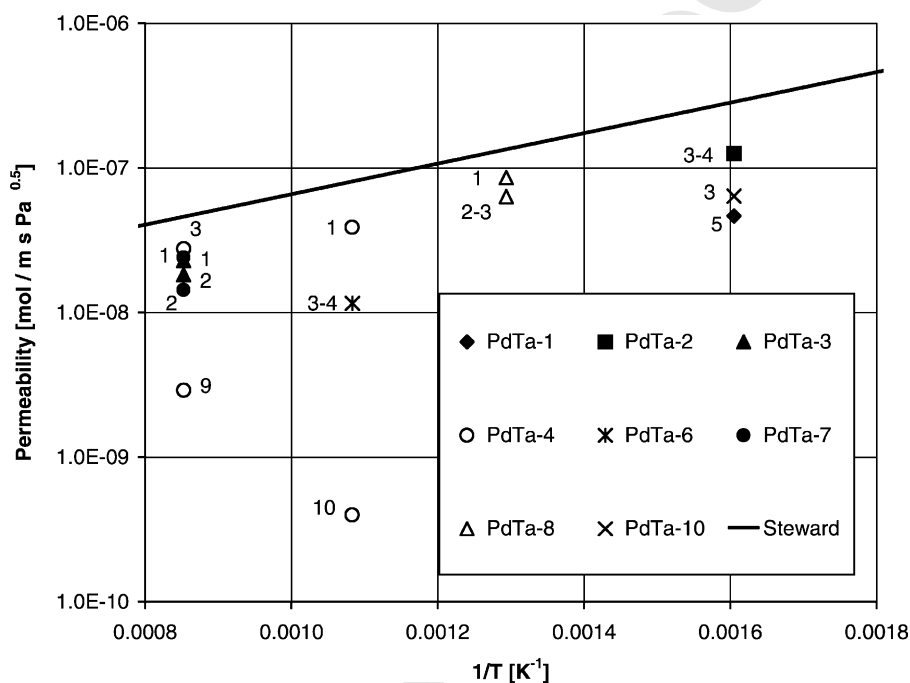


Fig. 10. Permeability of palladium sputter-coated over tantalum samples. Numbers in the legend correspond to membrane designations in the text and Table 1. Numbers near the data represent the number of days into test that the data point was acquired.

835 palladium-coated tantalum sample [15]. The delami- 870
 836 nation mechanism observed in this example is consis- 871
 837 tent with our other XPS observations that were never 872
 838 able to detect palladium dissolved in the bulk tanta- 873
 839 lum near the surface, suggesting that alloying was not 874
 840 a cause of palladium loss in these studies.

841 Permeation data collected during testing suggested 875
 842 that the palladium layer survived long enough to 876
 843 protect the tantalum surface from oxidation during 877
 844 heat-up and also provided a catalytic surface that 878
 845 enhanced permeation until its eventual demise. 879

846 4. Conclusions 880

847 A series of bulk tantalum and palladium-coated tan- 881
 848 talum membranes has been evaluated via direct per- 882
 849 meability testing in a flowing system, at temperatures 883
 850 from 623 to 1173 K, and hydrogen pressures from 0.1 884
 851 to 2.6 MPa. Membranes were characterized before and 885
 852 after testing so as to determine the effect of the test 886
 853 conditions on the sample surface. 887

854 All samples showed some degree of degradation and 888
 855 surface fouling, although the rates of degradation dif- 889
 856 fered for individual samples. It is likely that degrada- 890
 857 tion began immediately upon exposure to the high tem- 891
 858 peratures of study, although it usually manifested itself 892
 859 in experimental permeability measurements within a 893
 860 few days. 894

861 As expected, uncoated bulk tantalum fouled rela- 895
 862 tively quickly. This, combined with slow equilibration 896
 863 times, made meaningful data collection difficult. The 897
 864 tantalum coated with a 1 μm thick layer of palladium 898
 865 via electroless plating exhibited strength and tough- 899
 866 ness, experiencing temperatures up to 1173 K and to- 900
 867 tal pressure drops of up to 2.8 MPa over a 28-day 901
 868 period, but yielded the lowest overall permeabilities. 902
 869 This was attributed to the extensive handling that was 903
 904
 905
 906
 907

870 required during preparation and coating of the sam- 871
 872 ple. The sputter-coated samples gave the best overall 873
 874 results, at least over short periods of time. 875

876 Measured hydrogen permeabilities of tantalum and 877
 878 palladium-coated tantalum membranes approached, 879
 879 but never reached, the value predicted by the Stew- 880
 880 ard correlation. The highest absolute permeability 881
 881 was recorded on a sputter-coated, palladium-coated 882
 882 tantalum sample at 623 K. This condition also cor- 883
 883 responded with hydride formation and subsequent 884
 884 failure of the membrane. The highest value of per- 885
 885 meability as a percentage of that predicted by Stew- 886
 886 ard occurred before degradation of a thick sput- 887
 887 tered palladium-coated tantalum sample at 773 K. In 888
 888 general, the highest temperature of study, 1173 K, 889
 889 provided more consistent data with less scatter 890
 890 and slightly higher overall permeabilities relative 891
 891 to that of Steward than did the lower temperature 892
 892 conditions. 893

894 Fig. 11 shows the permeability values of both bulk 895
 895 tantalum and palladium-coated tantalum samples from 896
 896 this study recorded *within the first 5 days of testing*. 897
 897 Although the choice of 5 days is somewhat arbitrary, it 898
 898 encompasses enough points to be representative and is 899
 899 a short enough time period that *significant* degrada- 900
 900 tion had probably not yet set in. The resulting data, though 901
 901 still scattered, can be fit with an exponential expres- 902
 902 sion nearly parallel to that of Steward. Table 2 lists a 903
 903 pre-exponential constant of $4.2 \times 10^{-9} \text{ mol}/(\text{m s Pa}^{0.5})$ 904
 904 and an activation energy of -14.7 kJ/mol associated 905
 905 with the Arrhenius equation used to model the temper- 906
 906 ature dependence of this study, as well as those from 907
 907 previous literature references. The data shown here, in 908
 908 spite of the obvious shortcomings, would appear to at 909
 909 least qualitatively support the inverse temperature de- 910
 910 pendence of the Steward correlation over a wide range 911
 911 of temperature much more effectively than previous 912
 912 literature studies. 913

Table 2

Pre-exponential constant and activation energy for the hydrogen permeability of bulk tantalum and tantalum coated with thin palladium films

Membrane	Data	Reference	$X_{\text{M,Pd}}$ (μm)	T (K)	k_0 ($\text{mol}/(\text{m s Pa}^{0.5})$)	E/R (K)	E (kJ/mol)	R^2
Bulk Ta	Eq. (3)	[2] ^a	–	253–944 ^a	$5.8\text{E}-9$	–2430	–20.20	NA
Bulk Ta	Eq. (5)	[17]	–	948–1073	$1.0\text{E}-6$	3240	26.94	NA
Pd-coated Ta	Table 1 (8–13)	[13]	1–2	616–686	$5.2\text{E}-6$	2620	21.78	0.99
Bulk and Pd-coated Ta (first 5 days)	Table 1	This study	0–2	623–1173	$4.16\text{E}-9$	–1770	–14.71	0.29

^a Solubility and diffusivity data from temperatures of 624–944 and 253–573 K, respectively.

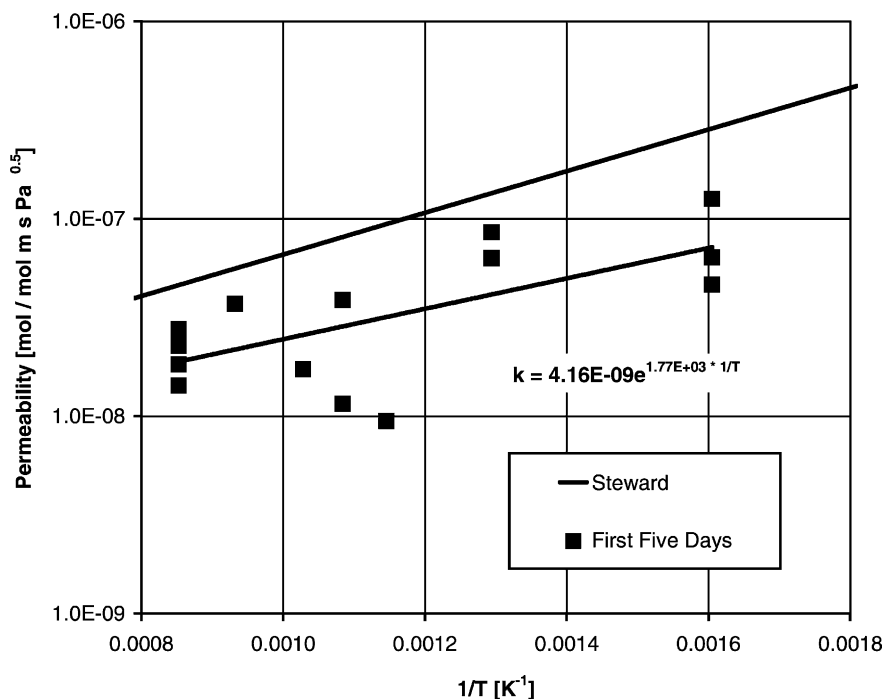


Fig. 11. Permeability values from bulk and palladium-coated tantalum recorded within the first 5 days of testing, compared to Steward correlation.

908 For the coated membranes, palladium was found to
 909 be lost from the tantalum surface for all samples stud-
 910 ied. One particularly interesting result showed peeling
 911 and flaking palladium following exposure to 773 K for
 912 49 h. This suggested that delamination, not interdiffu-
 913 sion, was the primary mechanism for palladium loss
 914 in samples at these conditions.

915 In spite of the efforts made to maintain a clean
 916 system, the testing was intended to simulate flowing
 917 conditions. Over the long durations of these tests,
 918 often a 100 h or more, even undetectable external
 919 leaks could have resulted in surface contamination
 920 and oxidation, which would in turn have increased
 921 surface resistance to the permeation of hydrogen.
 922 The methods employed to protect the tantalum sur-
 923 face from such contamination were only temporarily
 924 effective, at best, over the extreme conditions of
 925 study. As such, tantalum remains a promising ma-
 926 terial for hydrogen separation applications, but that
 927 promise will only be realized if more effective ways
 928 are found to protect the surface from fouling dur-
 929 ing the high-temperature, high-pressure, flowing gas

conditions of the next generation power and energy 930
 systems. 931

Acknowledgements 932

The hydrogen membrane testing unit at NETL was 933
 operated and maintained by the Engineering Techni- 934
 cians of Parsons Federal Services Inc., Ronald Hirsh, 935
 Paul Dieter, Ronald Benko, Jeremy Brannen, Michael 936
 Ditillo, Stephen Lopez, Brian Neel, and Raymond Ro- 937
 kicki. 938

Nomenclature

D (H_2/Ta)	diffusion coefficient of hydrogen atom in tantalum (m^2/s)
E	activation energy for membrane permeability (kJ/mol)
k	hydrogen permeability of metal ($mol/(m s Pa^{0.5})$)

k_0	hydrogen permeability constant (mol/(m s Pa ^{0.5}))
n	partial pressure exponent, 0.5–1.0
N_{H_2}	flux of hydrogen molecules (mol H ₂ /(m ² s))
P	total pressure (Pa)
P_{H_2}	hydrogen molecule partial pressure (Pa)
$P_{H_2,Perm}$	hydrogen molecule partial pressure on permeate side (Pa)
$P_{H_2,Ret}$	hydrogen molecule partial pressure on feed side (Pa)
R	gas constant (8.314 J/(mol K))
R^2	Pearson product moment correlation coefficient
S	hydrogen solubility (m ² /s)
T	temperature (K)
X_M	membrane thickness (m)

939 **References**

- 940 [1] R.M. Enick, B.D. Morreale, J. Hill, K.S. Rothenberger, A.V.
941 Cugini, R.V. Siriwardane, J.A. Poston, U. Balachandran, T.H.
942 Lee, S.E. Dorris, W.J. Graham, B.H. Howard, Evaluation and
943 Modeling of a High-Temperature, High-Pressure, Hydrogen
944 Separation Membrane for Enhanced Hydrogen Production
945 from the Water-Gas Shift Reaction, *Advances in Hydrogen*,
946 Kluwer Academic Publishers/Plenum Press, New York, 2000,
947 pp. 93–100.
- 948 [2] S.A. Steward, Review of Hydrogen Isotope Permeability
949 Through Metals, Lawrence Livermore National Laboratory
950 Report UCRL-53441, 15 August 1983.
- 951 [3] N. Boes, H. Zuchner, Diffusion of Hydrogen and Deuterium
952 in Ta, Nb, and V, *Phys. Status Solidi A* 17 (1973) K111–
953 K114.
- 954 [4] E. Veleckis, R. Edwards, *J. Phys. Chem.* 73 (3) (1969) 683.
- 955 [5] G. Schaumann, J. Volkl, G. Alefeld, *Phys. Status Solidi* 42
956 (1970) 401.
- [6] J. Volkl, G. Alefeld, Hydrogen diffusion in metals, in:
A.S. Nowick, J.J. Burton (Eds.), *Diffusion in Solids*,
Recent Developments, Academic Press, New York, 1975,
pp. 232–295. 957–959
- [7] B. Merisov, V. Khotkevitch, A. Karnus, *Phys. Metals
Metallogr.* 22 (1966) 163. 960–962
- [8] E. Wicke, A. Obermann, *Z. Phys. Chem. N. F.* 77 (1972) 163. 963
- [9] H. Zuchner, *Z. Phys. Chem. N. F.* 82 (1972) 240. 964
- [10] R. Cantelli, F. Mazzolai, M. Nuovo, *J. Phys. (Paris)* 32 (1971)
C2–C59. 965–966
- [11] B. Merisov, A. Serdyuk, I. Fal'ko, G. Khadzhay, V.
Khotkevitch, *Phys. Metals Metallogr.* 32 (1971) 154. 967–968
- [12] L. DeGraff, J. Rush, R. Livingston, H. Flotow, J. Rowe,
in: *Proceedings of the Sixth Jul-Conference, Jul-Ber.*, vol. 1,
1972, p. 301. 969–971
- [13] R.E. Buxbaum, T.L. Marker, Hydrogen transport through
non-porous membranes of palladium-coated niobium, *J.
Membr. Sci.* 85 (1993) 29–38. 972–974
- [14] R.E. Buxbaum, A.B. Kinney, Hydrogen transport through
tubular membranes of palladium-coated tantalum and
niobium, *Ind. Eng. Chem. Res.* 35 (1996) 530–537. 975–977
- [15] N.M. Peachey, R.C. Snow, R.C. Dye, Composite Pd/Ta
membranes for hydrogen separation, *J. Membr. Sci.* 111
(1996) 123–133. 978–980
- [16] T.S. Moss, N.M. Peachey, R.C. Snow, R.C. Dye, Multilayer
metal membranes for hydrogen separation, *Int. J. Hydrogen
Energy* 23 (2) (1998) 99–106. 981–983
- [17] A. Makrides, M. Wright, R. McNeill, Final Report Contract
DA-49-189-AMC-136(d), Tyco Lab, Waltham, MA, 1965. 984–985
- [18] M.A. Pick, J.W. Davenport, M. Strongin, G.J. Dienes,
Enhancement of uptake rates for Nb and Ta by thin surface
overlayers, *Phys. Rev. Lett.* 43 (4) (1979) 286–289. 986–988
- [19] R.E. Buxbaum, C.Z. Hsu, Methods for Plating Palladium, US
Patent 5,149,429, 22 September 1992. 989–990
- [20] C. Hsu, R.E. Buxbaum, Electroless and immersion plating
of palladium on zirconium, *J. Electrochem. Soc.* 132 (10)
(1985) 2419–2420. 991–993
- [21] K.S. Rothenberger, A.V. Cugini, R.V. Siriwardane, D.V.
Martello, J.A. Poston, E.P. Fisher, W.J. Graham, U.
Balachandran, S.E. Dorris, Performance testing of hydrogen
transport membranes at elevated temperatures and pressures,
Am. Chem. Soc., Fuel Chem. Div., Prepr. Pap. 44 (4) (1999)
914–918. 994–999